Role of Nonequilibrium Water Vapor Diffusion in Thermal Energy Storage Systems in the Vadose Zone

T. Başer, Ph.D., A.M.ASCE[1]; Y. Dong, Ph.D., A.M.ASCE[2]; A. M. Moradi, Ph.D.[3]; N. Lu, Ph.D., F.ASCE[4]; K. Smits, Ph.D.[5]; S. Ge, Ph.D.[6]; D. Tartakovsky, Ph.D.[7]; and J. S. McCartney, Ph.D., P.E., M.ASCE[8]

Abstract: Although siting of thermal energy storage systems in the vadose zone may be beneficial due to the low thermal conductivity of unsaturated soils, water phase change and vapor diffusion in soils surrounding geothermal heat exchangers may play important roles in both the heat injection and retention processes that are not considered in established design models for these systems. To better understand these roles, this study incorporates recently-developed coupled thermohydraulic constitutive relationships for unsaturated soils into a coupled heat transfer and water flow model that considers time-dependent, nonequilibrium water phase change and enhanced vapor diffusion. After calibration of key parameters using a tank-scale heating test on compacted silt, the subsurface response during 90 days of heat injection from a geothermal heat exchanger followed by 90 days of ambient cooling was investigated. Significant decreases in degree of saturation and thermal conductivity of the ground surrounding the heat exchanger were observed during the heat injection period that were not recovered during the cooling period. This effect can lead to a greater amount of heat retained in the ground beyond that estimated in conduction-based design models. **DOI: 10.1061/(ASCE)GT.1943-5606.0001910.**

Introduction

An important challenge facing society is the storage of energy collected from renewable sources. One such application is the storage of heat collected from solar thermal panels in the subsurface so that it can be harvested later (Claesson and Hellström 1981; Nordell and Hellström 2000; Chapuis and Bernier 2009). A practical mode of heat injection into the subsurface involves the circulation of a heated carrier fluid through a closely-spaced array of closed-loop geothermal heat exchangers in boreholes to reach ground temperatures ranging from 35 to 80°C (Sibbitt et al. 2012; Başer et al. 2016b; McCartney et al. 2017). Unsaturated soils in the vadose zone are an ideal thermal energy storage medium because the volume is abundant and low heat losses can be expected due to the lower thermal conductivity of soils when unsaturated (McCartney et al. 2013; Dong et al. 2015). The mode of heat transfer during injection of heat into unsaturated soils is complex as it may be coupled with thermally-induced water flow in either liquid or vapor forms along with latent heat transfer associated with phase change. However, most design models for geothermal heat storage systems focus on ground temperature changes during heating and do not consider coupled heat transfer and water transport (Claesson and Hellström 1981; Eskilson 1987). Although some recent studies on geothermal heat storage systems highlighted the importance of considering coupled heat transfer and water flow in their performance evaluation (Catolico et al. 2016; Moradi et al. 2016), the impact of water vapor diffusion and phase change during heat injection on the heat retention during a subsequent ambient cooling phase is an important topic that has not been investigated. This paper presents an evaluation of the response of a low-permeability, inactive, unsaturated silt layer surrounding a single geothermal heat exchanger to understand the impact of considering water vapor diffusion and phase change between liquid and water on the transient heat injection and retention processes. Comparison of the simulation results with a simpler model without water vapor diffusion or phase change permits an evaluation of the importance of these heat transfer mechanisms in simulating thermal energy storage systems in the vadose zone.

Background

Most models of heat transfer from geothermal heat exchangers employ analytical solutions to the heat equation assuming conduction is the primary mechanism of heat transfer, with constant

[1]Research Associate, Dept. of Civil and Environmental Engineering, Univ. of Alberta, 9211—116 St., NW Edmonton, AB, Canada T6G 1H9. Email: tugce@ualberta.ca

[2]Associate Professor, State Key Laboratory of Geomechanics and Geotechnical Engineering, Institute of Rock and Soil Mechanics, Chinese Academy of Sciences, Wuhan, Hubei 430071, China. Email: ydong@whrsm.ac.cn

[3]Research Associate, Dept. of Civil and Environmental Engineering, Center for Experimental Study of Subsurface Environmental Processes, Colorado School of Mines, 1500 Illinois St., Golden, CO 80401. Email: amoradig@mines.edu

[4]Professor, Dept. of Civil and Environmental Engineering, Colorado School of Mines, 1500 Illinois St., Golden, CO 80401. Email: ninglu@mines.edu

[5]Assistant Professor, Dept. of Civil and Environmental Engineering, Center for Experimental Study of Subsurface Environmental Processes, Colorado School of Mines, 1500 Illinois St., Golden, CO 80401. Email: ksmits@mines.edu

[6]Professor, Dept. of Geosciences, Univ. of Colorado Boulder, Boulder, CO 80309-0399. Email: Shemin.Ge@colorado.edu

[7]Professor, Dept. of Energy Resources Engineering, Stanford Univ., 367 Panama St., Stanford, CA 94305. Email: tartakovsky@stanford.edu

[8]Associate Professor, Dept. of Structural Engineering, Univ. of California San Diego, 9500 Gilman Dr., La Jolla, CA 92093-0085 (corresponding author). Email: mccartney@ucsd.edu

Note. This manuscript was submitted on February 2, 2017; approved on January 22, 2018; published online on May 3, 2018. Discussion period open until October 3, 2018; separate discussions must be submitted for individual papers. This paper is part of the ***Journal of Geotechnical and Geoenvironmental Engineering***, © ASCE, ISSN 1090-0241.

soil thermal properties (e.g., Kavanaugh 1998; Eskilson 1987; Yavuzturk 1999). Analytical solutions have been developed for heat exchanger geometries including the infinite line source (Ingersoll and Plass 1948; Beier et al. 2014), finite line source (Acuña et al. 2012; Lamarche and Beauchamp 2007), hollow cylinder source (Ingersoll et al. 1954; Gehlin 2002), finite plate source (Ciriello et al. 2015), and one- and two-dimensional solid cylinder sources (Tarn and Wang 2004). Although numerical simulations of geothermal heat exchangers have also been performed, most have also considered conduction as the primary mechanism of heat transfer in soils (Ozudogru et al. 2015; Welsch et al. 2015; Başer et al. 2016b). While these conduction-based analytical models and numerical simulations may be practical for the design of heat exchangers in dry or saturated low permeability soils, they may not be practical for design of those in unsaturated soils due to the potential for convective heat transfer associated with thermally-induced liquid water or water vapor flow, which may result in irreversible changes in behavior during cyclic heat injection and extraction. Further, the thermal properties of unsaturated soils are highly dependent on the degree of saturation, even when conduction is assumed to be the primary mode of heat transfer (e.g., Farouki 1981; Côté and Konrad 2005; Smits et al. 2013; Lu and Dong 2015). Conduction-only models may also not be practical for use in saturated soils with high permeability due to the potential for thermally induced convection of water from buoyancy effects (Catolico et al. 2016).

Because the properties of water in liquid and gas forms are dependent on temperature, heat transfer in the unsaturated soils in the vadose zone leads to thermally-induced water through soil. Specifically, temperature dependency of the density of liquid water ρ_w (Hillel 1980), dynamic viscosity of liquid water μ_w (Lide 2001), surface tension of soil water σ (Saito et al. 2006), relative humidity at equilibrium $R_{h,eq}$ (Philip and de Vries 1957), saturated vapor concentration in the gas phase $c_{v,sat}$ (Campbell 1985), vapor diffusion coefficient in air D_v (Campbell 1985), and the latent heat of water vaporization L_w (Monteith and Unworth 1990) may lead to thermally-induced water flow through unsaturated soils. The movement of water in soil caused by thermal and hydraulic gradients and the associated impacts on heat transfer have been studied experimentally for more than 100 years (Bouyoucos 1915; Smith 1943; Gurr et al. 1952; Baladi et al. 1981; Shah et al. 1984; Ewen 1988; Gens et al. 1998, 2007, 2009; Cleall et al. 2011; Smits et al. 2011; Moradi et al. 2015, 2016; Başer et al. 2016c). Some general observations from these studies are (1) heat transfer occurs in unsaturated porous media by conduction, convection in both liquid and gas phases, and latent heat transfer associated with water phase change; (2) water movement due to a temperature gradient is controlled by both vaporization/condensation processes as well as development of suction gradients caused by changes in water properties with temperature (i.e., density, viscosity, and solid-liquid contact angle) and drying effects; (3) vapor diffusion may occur at greater rates than that predicted by Fick's law; (4) the magnitude of thermally induced water flow depends on the initial degree of saturation; and (5) the times required to reach steady-state distributions in degree of saturation and temperature may be different depending on the coupling between the thermal and hydraulic properties of a given soil.

The governing equations for coupled heat transfer and flow of water in liquid and vapor forms have been investigated for unsaturated porous media in nondeformable conditions (Philip and de Vries 1957; Ewen and Thomas 1989; Thomas and King 1991; Thomas and Sansom 1995; Thomas et al. 2001; Smits et al. 2011), deformable conditions (Thomas and He 1997; Thomas et al. 1996), and in the presence of pore fluids containing salts or chemicals (Cleall et al. 2007; Olivella et al. 1996; Guimaraes et al. 2007, 2013). Most models for coupled heat transfer and water flow in liquid and vapor forms in nondeformable unsaturated soils are based on the model of Philip and de Vries (1957), who proposed the liquid island theory as an explanation for observations from studies like Gurr et al. (1952) that vapor diffusion occurred at a faster rate than predicted by Fick's law. Their theory is a pore-scale explanation where local thermal gradients is assumed to be higher across microscopic air-filled pores than the global thermal gradient across a soil element, and where water vapor diffusion is enhanced by evaporation and condensation from water held between soil particles by capillarity (liquid islands), effectively increasing the area available for vapor diffusion through a soil element. They implemented their pore-scale theory on a macroscopic scale by extending the vapor diffusion theory of Penman (1940) through inclusion of a soil-specific enhancement factor to correct the vapor diffusion rate calculated from Fick's law. Cass et al. (1984) found that the enhancement factor approaches 1.0 (no enhancement) for dry soils and increases significantly with increasing degree of saturation. Although the model of Philip and de Vries (1957) has been used in many coupled heat transfer and water flow problems in nondeformable soils, their model does not account for convective transport in the gas or liquid water phases, nonequilibrium phase change, vapor dispersion, or sensible heat dispersion in the liquid phase (Smits et al. 2011). Of these issues, consideration of nonequilibrium phase change in the model is expected to lead to more accurate identification of the appropriate vapor enhancement factor for a given soil (Smits et al. 2011). Lozano et al. (2008) observed that phase change may become the process limiting evaporation at low saturations rather than vapor diffusion as classically believed.

In the model of Philip and de Vries (1957), it is assumed that the water in liquid and gas phases are in equilibrium, which means that phase change occurs instantaneously in response to a change in vapor pressure. However, experimental studies have identified that time is required for liquid water to volatilize in response to a change in vapor pressure in a pore resulting from vapor diffusion in response to gradients in vapor pressure and/or temperature (Benet and Jouanna 1982; Armstrong et al. 1994; Chammari et al. 2008; Benet et al. 2009). To account for this in a model of coupled heat transfer and water flow, a source term for the liquid/gas phase change rate is added to the mass balance equations of liquid and vapor that is based on irreversible thermodynamics, first order reaction kinetics, or the kinetic theory of gases and contains a fitting coefficient that can calibrated for a given soil (Bénet and Jouanna 1982; Bixler 1985; Zhang and Datta 2004). Smits et al. (2011) adopted the source term of Bixler (1985) because it was derived from the kinetic theory of gases and is thus inherently temperature dependent. In the model of Bixler (1985), the vaporization rate is proportional to the difference between local equilibrium vapor pressure and local partial vapor pressure and the difference between the local degree of saturation and residual saturation. Smits et al. (2011) compared predictions of coupled heat transfer and water flow from equilibrium and nonequilibrium models, and found major differences in the early stages of the flow process, with greater differences for soils with initially lower degrees of saturation. Smits et al. (2011) and Trautz et al. (2015) also found that nonequilibrium models provide a better match to experimental data from column tests involving evaporation from fine sand with a heated surface than the model of Philip and de Vries, indicating that the nonequilibrium assumption for phase change may better capture the transient process of thermally-induced drying.

Model

Model Description

A nonequilibrium, nonisothermal, and coupled heat transfer and water flow numerical model developed by Smits et al. (2011) and extended by Moradi et al. (2016) was used to consider the behavior of an unsaturated soil layer during heating and cooling of a single vertical geothermal heat exchanger. The governing equation for nonisothermal liquid flow is given as follows (Bear 1972; Moradi et al. 2016):

$$nS_{rw}\frac{\partial \rho_w}{\partial t} + n\rho_w \frac{dS_{rw}}{dP_c}\frac{\partial P_c}{\partial t} + \nabla \cdot \left[\rho_w\left(-\frac{k_{rw}\kappa}{\mu_w}\right)\nabla(P_w + \rho_w g z)\right] = -R_{gw} \quad (1)$$

where n = porosity (m^3/m^3); S_{rw} = degree of water saturation (m^3/m^3); ρ_w = temperature-dependent density of water (kg/m^3) (Hillel 1980); t = time(s); $P_c = P_w - P_g$ = capillary pressure (Pa); P_w = pore water pressure (Pa); P_g = pore gas pressure (Pa); k_{rw} = relative permeability function for water (m/s); κ = intrinsic permeability (m^2); μ_w = temperature-dependent water dynamic viscosity (kg/ms) (Lide 2001); g = acceleration due to gravity (m/s^2); and R_{gw} = phase change rate (kg/m^3 s). Similarly, the governing equation for nonisothermal gas flow is given as follows (Bear 1972; Moradi et al. 2016):

$$nS_{rg}\frac{\partial \rho_g}{\partial t} + n\rho_g \frac{dS_{rg}}{dP_c}\frac{\partial P_c}{\partial t} + \nabla \cdot \left[\rho_g\left(-\frac{k_{rg}\kappa}{\mu_g}\right)\nabla(P_g + \rho_g g z)\right] = R_{gw} \quad (2)$$

where S_{rg} = degree of gas saturation (m^3/m^3); ρ_g = temperature-dependent density of gas (kg/m^3) (Smits et al. 2011); k_{rg} = relative permeability function for gas (m/s); and μ_g = temperature-dependent gas dynamic viscosity [kg/(ms)]. The water vapor mass balance equation is given as follows (Smits et al. 2011):

$$n\frac{\partial(\rho_g S_{rg} w_v)}{\partial t} + \nabla \cdot (\rho_g u_g w_v - D_e \rho_g \nabla w_v) = R_{gw} \quad (3)$$

where $D_e = D_v\tau$ = effective diffusion coefficient (m^2/s); D_v = diffusion coefficient of water vapor in air (m^2/s) (Campbell 1985); w_v = mass fraction of water vapor in the gas phase (kg/kg); and $\tau = n^{1/3}S_{rg}^{7/3}\eta$ = tortuosity (Millington and Quirk 1961). The value of η is the enhancement factor for vapor diffusion defined using the model of Cass et al. (1984):

$$\eta = a + 3S_{rw} - (a-1)\exp\left\{-\left[\left(1 + \frac{2.6}{\sqrt{f_c}}\right)S_{rw}\right]^3\right\} \quad (4)$$

where a = empirical fitting parameter; and f_c = clay content. The nonequilibrium gas phase change rate is calculated as follows (Bixler 1985; Zhang and Datta 2004; Moradi et al. 2016):

$$R_{gw} = \left(\frac{bS_{rw}RT}{M_w}\right)(\rho_{veq} - \rho_v) \quad (5)$$

where b = empirical fitting parameter (s/m^2); R = universal gas constant (J/molK); $\rho_{veq} = c_{v,sat}R_{h,eq}$ = equilibrium vapor density (kg/m^3); T = temperature (K); $\rho_v = \rho_g w_v$ = vapor density (kg/m^3); and M_w = molecular weight of water (kg/mol). Finally, the heat transfer energy balance is given as follows (Whitaker 1977; Moradi et al. 2016):

$$(\rho C_p)\frac{\partial T}{\partial t} + \nabla \cdot ((\rho_w C_{pw})u_w T + (\rho_g C_{pg})u_g T - (\lambda \nabla T)) = -L_w R_{gw} + Q \quad (6)$$

where ρ = total density of soil (kg/m^3); C_p = specific heat of soil (J/kgK); C_{pw} = specific heat capacity of water (J/kgK); C_{pg} = specific heat capacity of gas (J/kgK); λ = thermal conductivity (W/mK); L_w = latent heat of water vaporization (J/kg); u_w = water velocity (m/s); u_g = gas velocity (m/s); and Q = heat source (W/m^3). The system of partial differential equations given in Eqs. (1)–(6) was solved simultaneously using COMSOL Multiphysics software.

Calibration of the model requires soil-specific quantification of the parameters for the thermohydraulic constitutive relationships governing water retention, hydraulic conductivity, thermal conductivity, and volumetric heat capacity, as well as estimates of parameters a and b in Eqs. (4) and (5) that govern the rates of vapor diffusion and phase change, respectively. The model used in the simulations incorporates recently-developed thermohydraulic constitutive relationships for unsaturated soils (Lu and Dong 2015; Baser et al. 2016a). The experimental approach used by Lu and Dong (2015) was used to obtain the data for calibration of these coupled thermohydraulic constitutive relationships. Lu and Dong (2015) used a modified form of the transient-release and imbibition method (TRIM) of Wayllace and Lu (2012) that included a dual-needle thermal probe to measure the thermal conductivity and volumetric heat capacity during monotonic drying of different unsaturated soils under isothermal conditions. TRIM uses an inverse analysis to estimate the parameters of the soil-water retention curve (SWRC) and hydraulic conductivity function (HCF) given by van Genuchten (1980). These parameters include α_{vG}, which represents the inverse of the air entry suction in the SWRC; N_{vG}, which represents the pore size distribution in the SWRC; and k_{sw}, which is the hydraulic conductivity of saturated soil. The value of k_{sw} obtained from a test at room temperature can be used to calculate the intrinsic permeability κ in Eq. (1). Although the saturation-dependent relative permeability to water (the HCF) was assumed not to vary with temperature, the hydraulic conductivity of the unsaturated soil will vary with temperature because the dynamic viscosity and density of water vary with temperature according to the relationships presented in Lide (2001) and Hillel (1980), respectively. The relative permeability to gas was not measured in this study but was assumed to equal $k_{rg} = 1 - k_{rw}$. The temperature-dependent surface tension σ relationship presented by Saito et al. (2006) was used in the temperature correction for capillary pressure of Grant and Salehzadeh (1996), given as follows:

$$P_c(T) = P_c(T_{ref})[\sigma(T)/\sigma(T_{ref})] \quad (7)$$

where σ = surface tension (N/m); T = temperature (K); and T_{ref} = initial reference temperature of 293.15 K.

Lu and Dong (2015) defined a thermal conductivity function (TCF) that is able to capture transitions in the thermal conductivity in the capillary, funicular, and pendular water retention regimes of the SWRC, given as follows:

$$\frac{\lambda - \lambda_{\text{dry}}}{\lambda_{sat} - \lambda_{\text{dry}}} = 1 - \left[1 + \left(\frac{S_{rw}}{S_{\text{f}}}\right)^m\right]^{1/m-1} \quad (8)$$

where λ_{dry} and λ_{sat} = thermal conductivities of dry and saturated soil specimens, respectively; S_f = parameter representing the degree of saturation at the onset of the funicular regime; and m = parameter related to the pore fluid network connectivity.

Lu and Dong (2015) correlated the parameters of the TCFs and SWRCs of several soils and found that the m parameter in the TCF is related to the pore-size parameter N_{vG} in the SWRC model of van Genuchten (1980), and can be estimated to be 3.0 to $0.2N_{vG}$. Evaluation of the form of Eq. (8) indicates that the thermal conductivity will not reduce to the value of λ_{sat} when $S_e = 1$, so Lu and Dong (2015) treated λ_{sat} as a fitting parameter.

Başer et al. (2016a) presented trends in the volumetric heat capacity of compacted silt during monotonic drying and found that it also depends on the degree of saturation in a similar manner to the thermal conductivity, and defined a volumetric heat capacity function (VHCF) that has the same form as the THF of Lu and Dong (2015), as follows:

$$\frac{C_v - C_{v\text{dry}}}{C_{vsat} - C_{v\text{dry}}} = 1 - \left[1 + \left(\frac{S_{rw}}{S_\text{f}}\right)^m\right]^{1/m-1} \tag{9}$$

where C_{vdry} and C_{vsat} = volumetric heat capacities of dry and saturated soil, respectively, and are similarly treated as fitting parameters; and S_f and m are the same parameters as in Eq. (8). Başer et al. (2016a) found that this model and the assumptions regarding the parameters provided a good match to the volumetric heat capacity data measured in the TRIM tests on different soils performed by Lu and Dong (2015) that were not reported in their paper due to its focus on the thermal conductivity.

Although Smits et al. (2013) observed that the TCF may vary with temperature, this temperature dependency is likely due to vapor diffusion and phase change that was not accounted for in their simulations. Because the simulations in this study account for vapor diffusion and phase change explicitly, the TCF and VHCF measured at 20°C were used in the coupled heat transfer and water flow simulations

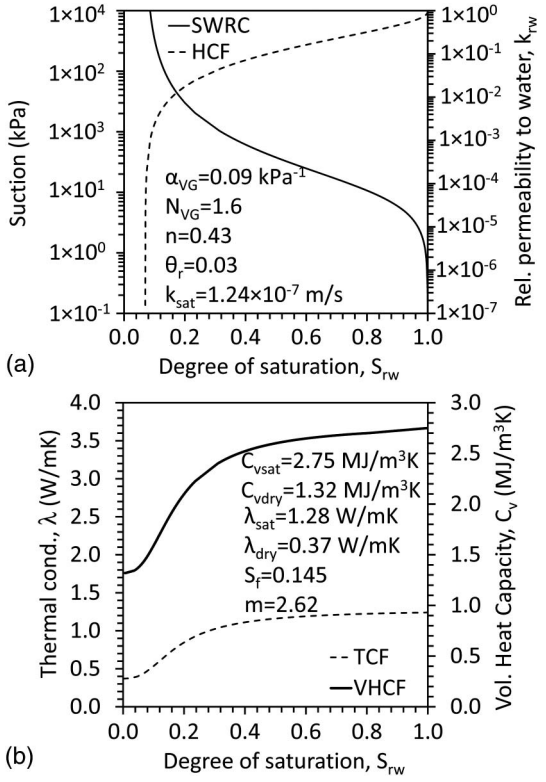

Fig. 1. Hydraulic and thermal constitutive relationships and relevant parameters for Bonny silt: (a) SWRC; (b) HCF; (c) TCF; and (d) VHCF.

Calibration of Thermohydraulic Constitutive Relationships

The soil investigated in this study is Bonny silt, which is classified as ML (inorganic silt) according to the Unified Soil Classification System (USCS) and has a specific gravity of 2.65. The soil specimens used in the calibration process were prepared using compaction at a gravimetric water content of 13.7% and a dry unit weight of 14.0 kN/m^3, which correspond to an initial degree of saturation of 0.42 and a porosity of 0.46. For reference, the optimum water content and the maximum dry unit weight corresponding to the standard Proctor compaction effort are 13.6% and 16.3 kN/m^3, respectively. Silt was selected for this evaluation because it is not expected to deform significantly during changes in temperature or degree of saturation, and it retains water under relatively high suctions. The latter point implies that the initial degree of saturation will vary along the length of a typical geothermal heat exchanger installed in an unsaturated Bonny silt layer.

The SWRC and HCF (in terms of the relative permeability to water) obtained from the modified TRIM test on compacted Bonny silt are shown in Fig. 1(a) along with the model parameters. The shape of the SWRC indicates that an appreciable amount of water will be retained in the soil several meters above the water table under hydrostatic conditions. The compaction conditions for these curves are the same as those mentioned previously, even though Lu and Dong (2015) report a different porosity due to a lower value of G_s used in their calculations. An intrinsic permeability of 1.27×10^{-14} m^2 was calculated from the hydraulic conductivity of saturated soil of 1.24×10^{-7} m/s from the values of water viscosity and density at 20°C (293.15 K). The TCF and VHCF for Bonny silt are shown in Fig. 1(b), along with the parameters given in Eqs. (8) and (9). The value of $m = 2.62$ measured in the experiment for Bonny silt was used in the simulations, which is lower than the value of 2.68 obtained from the correlation with N_{vG} of Lu and Dong (2015). The experimental value still reflects the coupling between the thermohydraulic properties as they were defined in the same test. The thermal conductivity varies from 1.25 to 0.37 W/mK for saturated to dry conditions, respectively, while the volumetric heat capacity varies from 2.75 to 1.30 MJ/m^{3}K for saturated to dry conditions, respectively. These variations with degree of saturation may lead to changes in heat retention if a soil experiences drying during heat injection.

Calibration of Vapor Diffusion and Phase Change Parameters

To define the parameters a and b, a tank-scale heat injection experiment was performed in an instrumented layer of compacted Bonny silt, which was then simulated using the parameters from the thermohydraulic constitutive relationships defined in Fig. 1. A schematic of the experimental setup is shown in Fig. 2. Bonny silt was compacted in nine lifts in a cylindrical aluminum container having a diameter of 550 mm and a height of 477 mm. A 215 mm-long cylindrical cartridge heater having a diameter of 10 mm was used as the heating source. During heat injection, a temperature control unit was used to impose a constant temperature boundary condition of 60°C on the heating rod. To monitor changes in temperature and degree of saturation during heating of the soil, a total of 10 5TM dielectric sensors manufactured by Decagon Devices of Pullman, WA were placed at the locations shown in Fig. 2. After all the lifts and sensors were placed, the top of the soil layer was covered with several layers of plastic wrap to minimize loss of water vapor to the laboratory air. The top and sides of the tank were then wrapped

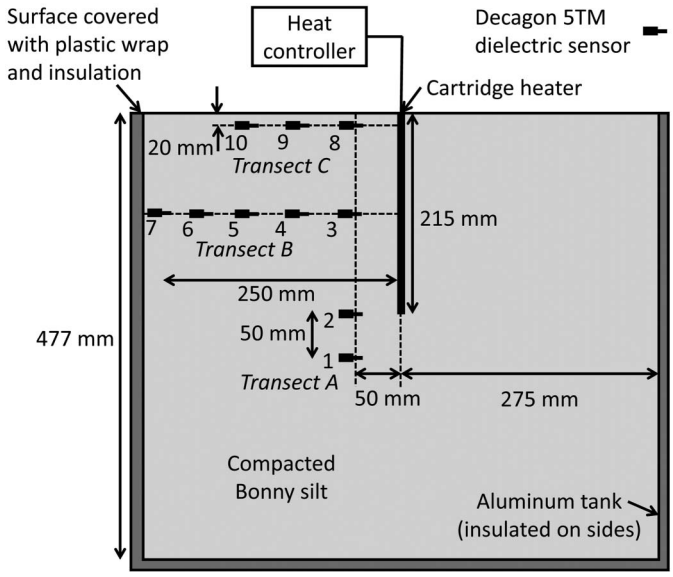

Fig. 2. Cross-sectional elevation view of the experimental setup for model calibration with dielectric sensor locations.

in insulation, and thermocouples were used to monitor the temperatures of the boundaries of the tank. The soil had an initial temperature of 23.5°C and an initial degree of saturation of 0.42.

In the simulations of the tank-scale tests, no mass flux boundary conditions were applied for both liquid water and vapor flow for all boundaries of the tank. The top boundary was thermally insulated, convective heat flux boundaries were defined for the side boundaries to consider heat loss from the insulated tank, a constant temperature boundary condition was used for the heating rod, and a constant temperature of 18°C was applied at the bottom of tank. Results from the numerical analyses were then compared with the experimental results to calibrate the parameters a and b. Comparisons of predicted and measured time series of temperature and degree of saturation inferred from dielectric Sensor #3 are shown in Figs. 3(a–d). Sensor #3 was selected as the primary location for calibration of the model as it is near the center of the heating rod and is relatively close to the heat exchanger. The predicted time series in these figures include curves for different values of the fitting parameters a and b. The parameters are observed to have a greater effect on the change in degree of saturation as they control the rates of vapor diffusion and water phase change. Simulations for no vapor diffusion or phase change are also shown in Figs. 3(a and b), which indicate slower increases in temperature to lower magnitudes at this location as well as a negligible change in degree of saturation. Values of $a = 30$ and $b = 5 \times 10^{-7}$ s/m^2 were found to best fit the data based on visual inspection, a similar approach used by Smits et al. (2011).

To evaluate the calibration, the spatial distributions of temperature and degree of saturation along Transects B and A at the end of the heating from the numerical simulations and the experiments are shown in Figs. 4(a–d). In most of the cases, the predicted profiles show good agreement with the measured data, except in the case of the degree of saturation measured by the sensor nearest the edge of container in Fig. 4(b). This sensor may have malfunctioned due to the compaction process. Overall, the temporal and spatial comparisons in Figs. 3 and 4 indicate that the calibrated values of a and b can be assumed to be representative of Bonny silt under these compaction conditions.

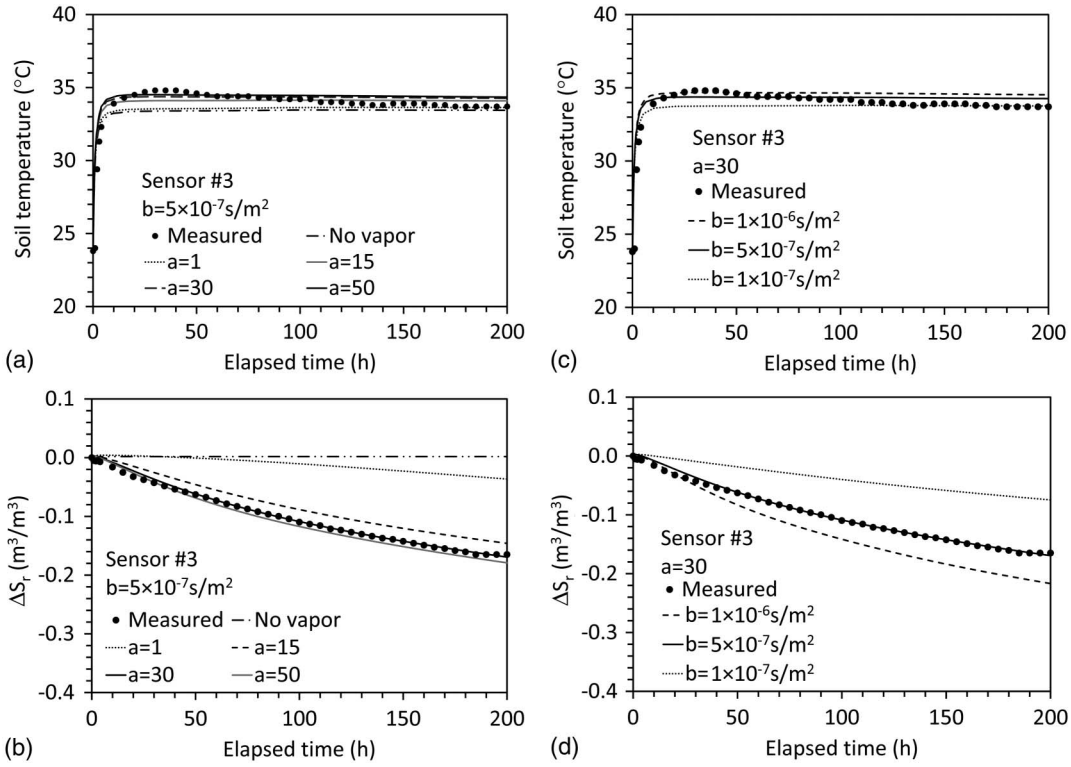

Fig. 3. Predicted and measured time series from the tank-scale heating test: (a) soil temperatures for different values of a; (b) changes in degree of saturation for different values of a; (c) soil temperatures for different values of b; and (d) changes in degree of saturation for different values of b.

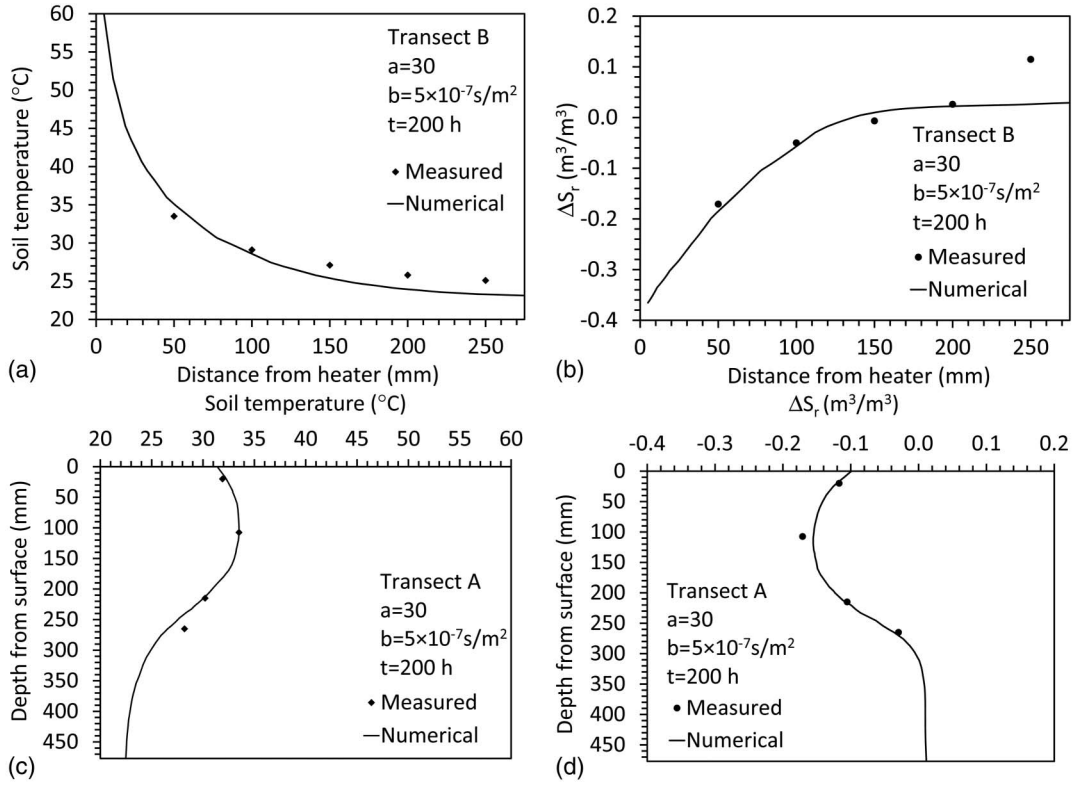

Fig. 4. Simulated and observed temperatures and changes in degree of saturation: (a) horizontal temperature profile; (b) horizontal change in degree of saturation profile; (c) vertical temperature profile; and (d) vertical change in degree of saturation profile.

Evaluation of Vapor Diffusion and Phase Change around a Field-Scale Geothermal Heat Exchanger

Scenario Considered

The primary goal of this study is to use the calibrated parameters to understand the changes in the behavior of a layer of unsaturated Bonny silt surrounding a geothermal heat exchanger during a heating and cooling cycle representative of geothermal heat storage systems. Although geothermal heat storage systems typically involve an array of geothermal heat exchangers with spacings as close at 1.5 m (Baser et al. 2016b), this study focuses on the changes in soil behavior around a single geothermal heat exchanger. This choice simplifies the boundary conditions and permits evaluation of the relative effects of the different heat transfer mechanisms. It is possible that the close spacing between geothermal heat exchangers may lead to different distributions in temperature and degree of saturation than those observed in this evaluation due to interactions between heat exchangers, but the simpler scenario of a single heat exchanger is evaluated in this paper to help establish the impact of a heating-cooling cycle on the distributions in temperature and degree of saturation in the surrounding unsaturated silt layer.

The geothermal heat exchanger investigated in this study has a length of 25 m and a radius of 0.04 m, embedded at a depth of 1 m from the surface. The embedment is consistent with the practice of installing geothermal heat exchangers below the frost depth. Even though this scenario could be investigated using an axisymmetric analysis, a 3D simulation was performed for a rectangular domain so that the domain could be modified to incorporate additional heat exchangers in future studies. The quarter domain having a height of 30 m and a width of 10 m with the geothermal heat exchanger along one edge is shown in Fig. 5. The entire domain was assumed to be uniform and isotropic, and the soil was discretized into 101,073 elements (394,394 degrees of freedom) with finer elements around the heat exchanger. The hydraulic and thermal boundary conditions for the models are also shown in Fig. 5. For liquid water and gas flow, Neumann boundary conditions (no mass flux) were assumed for all boundaries except the bottom boundary, which was set to be a constant head boundary condition corresponding to the water table. For heat transfer, a constant temperature that represents an average mean subsurface soil temperature of 21°C was applied at the bottom while at the outer boundaries the temperature varied with depth. No heat transfer boundary conditions were applied to the planes of symmetry. The size of the domain was selected to be large enough that on the outer vertical boundaries a constant temperature and zero fluid flux could be assumed.

The initial conditions are shown in the color bars in Fig. 5. The initial ambient temperature of the domain was assumed to be a function of depth until a certain depth of 9 m from surface, and this initial temperature profile is a representative of early summer months in San Diego (specifically May 2015). A hydrostatic initial condition was assumed, so the soil along the length of the heat exchanger is unsaturated with initial degrees of saturation ranging from 0.50 to 0.21 depending on the height from the water table. Two locations of interest that will be investigated further are noted in Fig. 5(b) having different initial degrees of saturation.

During heat injection, a constant heat flux of 50 W/m^2 was applied to the outer boundary of the geothermal heat exchanger. This heat flux was converted to a volumetric heat source to obtain the value of Q in Eq. (6). Although the magnitude of heat flux used in this study is representative of average value in thermal energy storage systems, a constant heat flux is not expected in a system where solar thermal panels are the heat source. In these cases, the heat

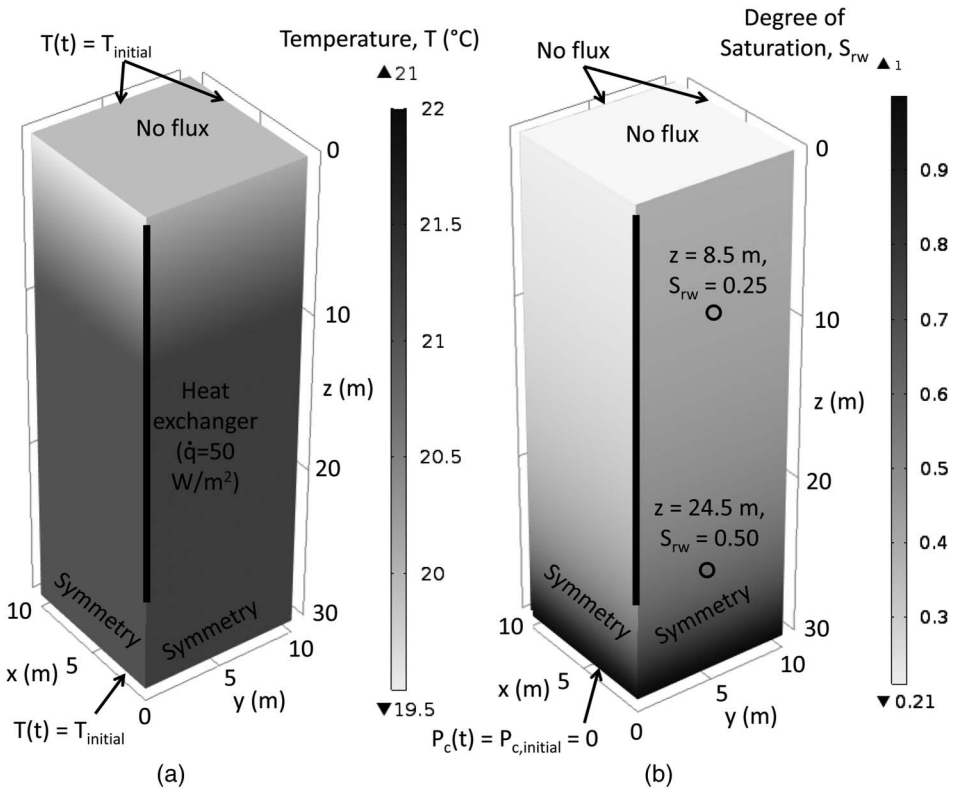

Fig. 5. Initial and boundary conditions on the quarter domain model for a field-scale geothermal heat exchanger: (a) thermal; and (b) hydraulic.

input from the solar thermal panels will remain relatively constant, which means that the heat flux will decrease with time as the subsurface warms (Welsch et al. 2015). Although use of a constant heat flux will lead to greater increases in ground temperature than those expected when using solar thermal panels as the heat source, it provides a simple boundary condition for evaluating the roles of different heat transfer mechanisms in unsaturated soils.

Heat Transfer and Water Flow Evaluation

The temperature time series at a distance of 0.05 m from the geothermal heat exchanger and a depth of 8.5 m from the surface (i.e., $S_{r0} = 0.25$) is shown in Fig. 6(a). After the 90-day heat injection period, a maximum temperature of 45.6°C is observed. For comparison, the temperature time series from a model with no water vapor (i.e., with no vapor diffusion or phase change, but with thermally-induced liquid water flow) is also shown in Fig. 6(a). In addition to showing a slower rate of increase in temperature, a lower maximum temperature of 36.3°C was observed for the model with no water vapor. After the heating injection period, the heat flux was set to 0 $\mathrm{W/m^2}$ and the soil was allowed to cool ambiently. After 180 days from the start of the simulation (90 days after the end of heat injection), the temperature decreased to 22.8°C for the model with vapor diffusion and phase change, but decreased at a faster rate to 21.9°C for the model with no vapor. The slower rate of cooling for the prior case is expected to be due to the decrease in degree of saturation of the soil due to vapor diffusion and latent heat transfer observed in Fig. 6(b). At the end of the heat injection period, a decrease in degree of saturation of 0.14 at this depth was observed for the model with vapor diffusion, while a negligible decrease in degree of saturation of 0.01 was observed for the model with no vapor. The greater decrease in the degree of saturation for the model with vapor diffusion and phase change led to a lower thermal conductivity according to the TCF (from 0.84 to 0.49 W/mK), which will be assessed in more detail later. Not only was the temperature higher near the heat exchanger for the model with vapor diffusion and latent heat transfer, but the lower thermal conductivity at the end of the heating period caused heat to dissipate at a slower rate during ambient cooling than for the model with no vapor. Another interesting observation from Fig. 6(b) is that at the end of the 90-day cooling period, only 16.5% of the decrease in degree of saturation observed during heat injection was recovered, indicating that the drying near the heat exchanger was permanent from a practical point of view. This may have an impact on subsequent heat injection and cooling cycles, and may be one of the reasons that an increase in the ground temperature is observed after several cycles of heat injection and extraction in practice (Sibbitt et al. 2012).

Radial distributions in temperature at a depth of 8.5 m from the surface at the ends of the heat injection and cooling periods are shown in Fig. 7(a). Heat injection led to a notable change in temperature up to a distance of about 3 m from the heat exchanger. The temperature at the location of the heat exchanger was nearly 10°C greater when vapor diffusion and latent heat transfer was considered than the case when it was not, and the temperature at the end of the ambient cooling period was greater throughout the zone of influence. A decrease in degree of saturation was only observed within approximately 1 m from heat exchanger for the model with vapor diffusion and phase change, as shown in Fig. 7(b). A slight decrease in degree of saturation was observed near the heat exchanger for the model with no vapor due to thermally-induced liquid flow. The zone of influence for temperature changes is greater than the zone of influence for degree of saturation changes for the conditions evaluated. For Bonny silt, this indicates that an

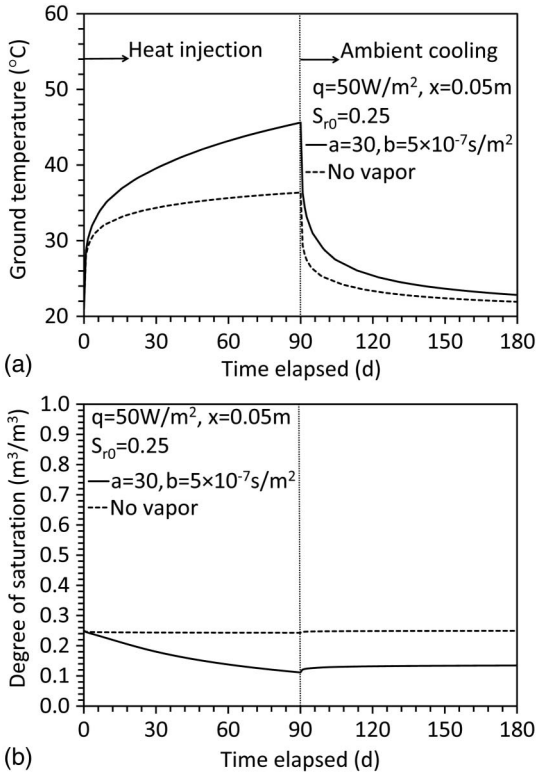

Fig. 6. Comparisons of the effects of heat transfer mechanisms and heat flux for a 90-day heat injection period followed by cooling: (a) temperature time series; and (b) degree of saturation time series.

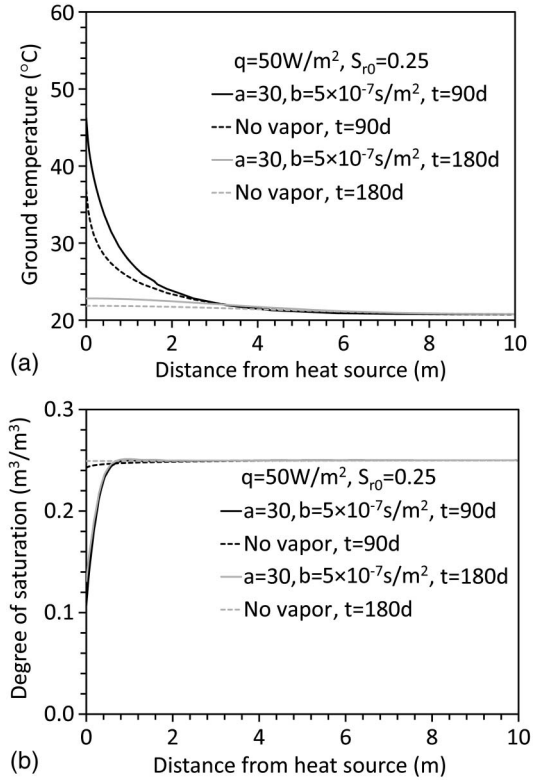

Fig. 7. Effects of including vapor flow in the coupled analysis at a depth of 9.5 m (an initial degree of saturation of 0.25): (a) radial profiles of temperature at the end of heating and cooling; (b) radial profiles of degree of saturation at the end of heating and cooling.

overlap in the effects of different heat exchangers may be observed for the typical geothermal heat exchanger spacing of 1.5 m in thermal energy storage systems.

Profiles of temperature with depth at horizontal distances of 0.05 and 0.20 m from the heat exchanger at the end the 90-day heat injection period are shown in Fig. 8(a). The temperature profiles varied nonlinearly with depth and had a maximum value at a depth of 4.5 m from the surface. For comparison, the temperature profiles for the model with no water vapor show more uniform distributions in temperature with depth at the end of the heat injection period. The difference in temperature observed with depth in both models is due to the thermohydraulic properties with depth associated with the variations in initial degree of saturation with depth shown in Fig. 5. A significant decrease in the degree of saturation with depth is observed at both horizontal distances for the model with vapor diffusion and phase change in Fig. 8(b), while only a slight decrease was observed for the model with no vapor. Profiles of temperature after the ambient cooling are shown in Fig. 8(c), with the profiles at horizontal distances of 0.05 and 0.20 m overlapping. Although most of the heat injected has dissipated away from the heat exchanger, more heat was retained in the soil for the model with vapor diffusion and phase change. The profiles of degree of saturation at the end of the cooling period shown in Fig. 8(d) only show slight increases from the profiles observed in Fig. 8(b).

The impact of the initial degree of saturation on heat transfer and water flow can be investigated by evaluating the transient response at different depths in the soil profile, which have different initial degrees of saturation. Time series of temperature at depths of 8.5 and 24.5 m from the surface at a horizontal distance of 0.05 m from the heat exchanger corresponding to initial degrees of saturation of 0.25 and 0.50 are shown in Fig. 9(a). Increases in temperature of 45.6 and 42.3°C at the end of the heat injection period were observed when the initial degree of saturation was doubled from 0.25 to 0.50. However, decreases in degree of saturation of 0.14 and 0.35 were observed at the end of the heat injection period for the same depths, as shown in Fig. 9(b). The greater decrease in degree of saturation for the initially wetter soil is likely due to the availability of water to evaporate from the region near the heat exchanger. The horizontal zone of influence of the change in temperature is similar for the two depths as shown in Fig. 9(c), but the horizontal zone of influence of the change in degree of saturation was greater at the depth of 8.5 m as shown in Fig. 9(d). This is consistent with observations that dryer initial conditions lead to greater zones of influence of vapor diffusion (e.g., Smits et al. 2011). The soil with $S_{r0} = 0.50$ also shows a slight wetting front due to the movement of water away from the heat exchanger.

Assessment of Heat Transfer Mechanisms and Effects of Coupled Flow

Profiles of the thermal conductivity and volumetric heat capacity values that correspond to the profiles of degrees of saturation in Fig. 8(b) are shown in Figs. 10(a and b), respectively. Despite the nonlinear decrease in degree of saturation along the length of the heat exchanger, a comparatively uniform decrease of approximately 0.3 W/mK is observed at 0.05 m from the heat exchanger. A more nonlinear decrease in thermal conductivity is observed further away from the heat exchanger at 0.20 m. The shapes of the profiles of the volumetric heat capacity are the same as those for the thermal conductivity due to the same parameters used in Eqs. (8) and (9), but because of the range of the two relationships for Bonny silt the volumetric heat capacity decreased by as much as 25% while the thermal conductivity decreased by as much as 70%. This is a positive finding for thermal energy storage in similar soil

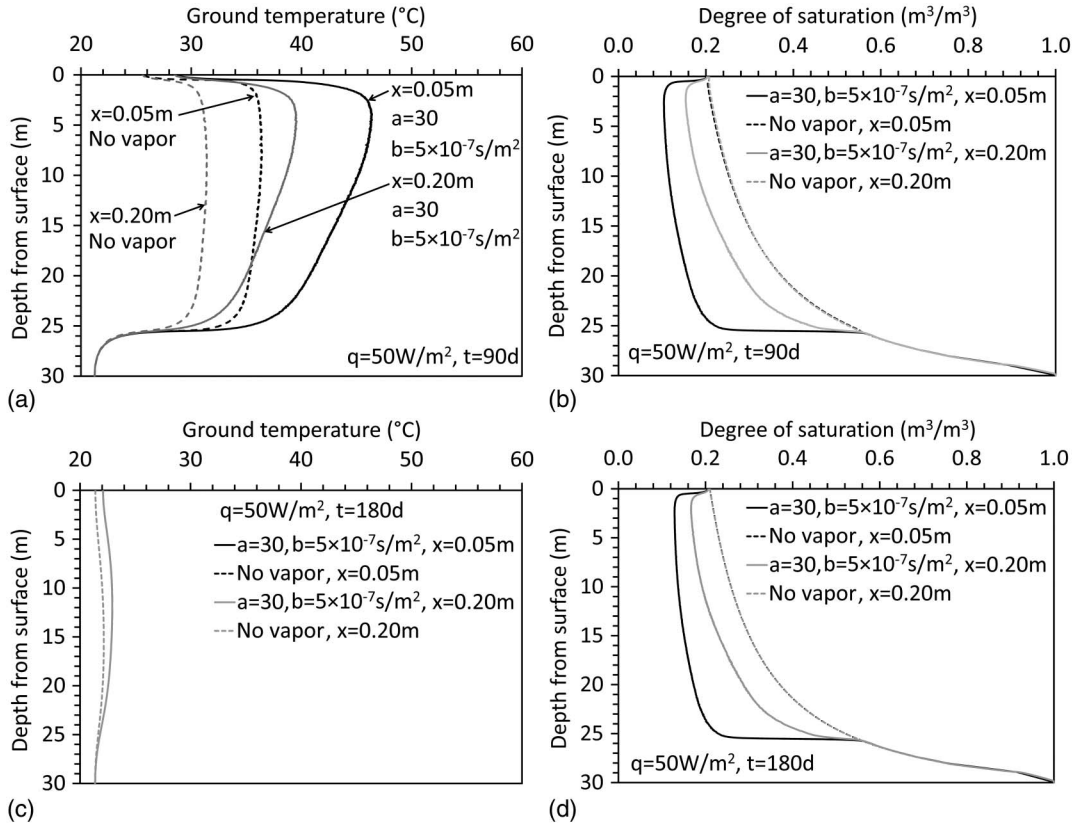

Fig. 8. Vertical profiles for comparison of different heat transfer mechanisms: (a) temperature at the end of a 90-day heat injection period; (b) degree of saturation at the end of a 90-day heat injection period; (c) temperature at the end of a 90-day cooling period; and (d) degree of saturation at the end of a 90-day cooling period.

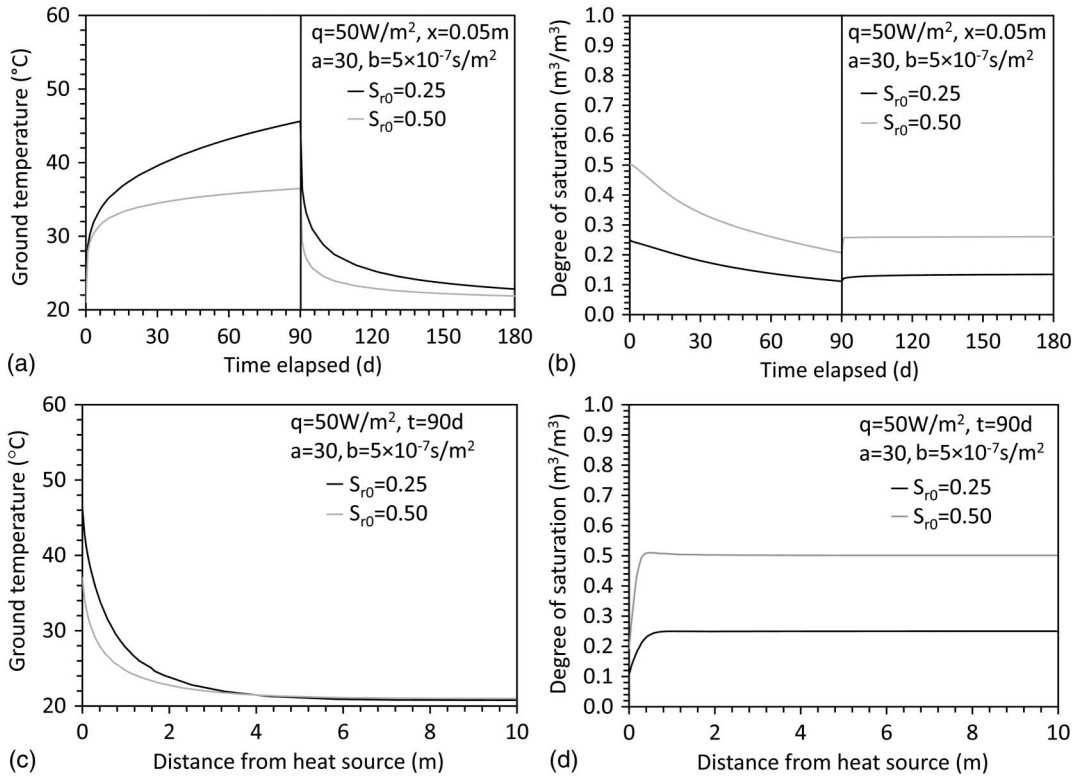

Fig. 9. Effect of initial degree of saturation: (a) time series of temperature; (b) time series of degree of saturation; (c) radial temperature profiles; and (d) radial degree of saturation profiles.

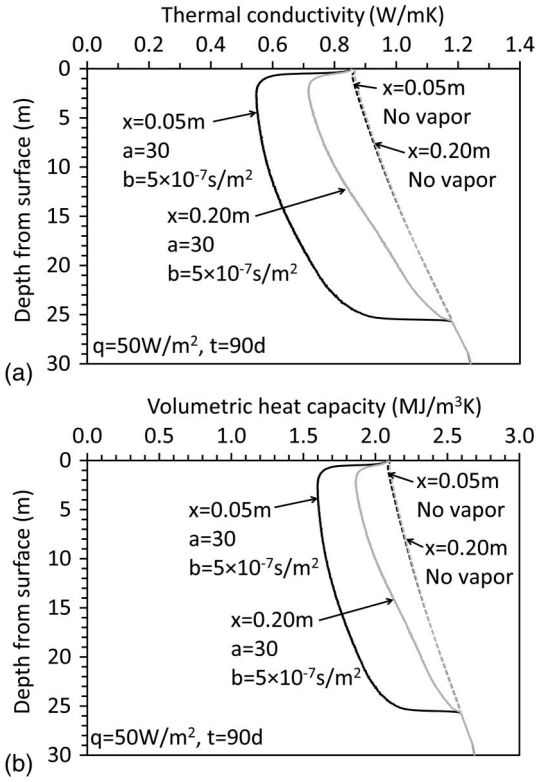

Fig. 10. Thermal property evaluation at the end of heat injection: (a) thermal conductivity profiles; and (b) volumetric heat capacity profiles.

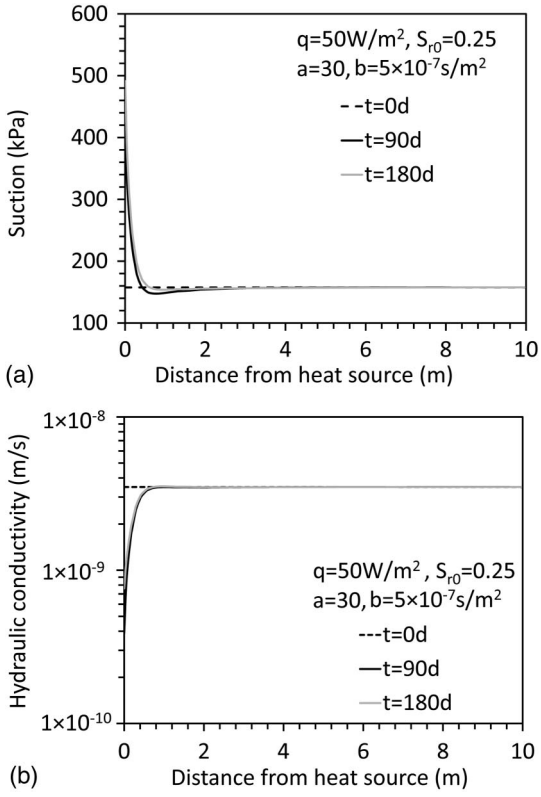

Fig. 11. Liquid water flow evaluation: (a) horizontal profiles of suction at different times; and (b) horizontal profiles of hydraulic conductivity at different times.

deposits, as it means that lower heat losses can be expected without a significant reduction in the quantity of heat stored.

The vapor diffusion and latent heat transfer that results in the drying around the heat exchanger also leads to a suction gradient that may result in liquid water flow back toward the heat exchanger. Horizontal profiles of suction profiles at a depth of 8.5 m ($S_{r0} = 0.25$) at different times are shown in Fig. 11(a). Large increases in suction are observed within 0.6 m from the heat exchanger, with decreases in suction beyond that point. Despite the large gradient associated with the suction distribution at the end of the heating period, the suction did not return to its original distribution during the ambient cooling period. This may have been due to the order of magnitude decrease in the hydraulic conductivity (adjusted for temperature effects) shown in Fig. 11(b), indicating that a longer duration may be needed for liquid flow to occur than permitted in the 90-day cooling period.

Vapor concentrations (kg/m^3) near the heat exchanger normalized by the equilibrium vapor concentration (kg/m^3) are shown in Fig. 12(a) for Bonny silt with initial degrees of saturation of 0.25 and 0.50 (depths of 8.5 and 24.5 m). When the normalized vapor concentration is greater or equal to 0.75, the phase change in the soil can be assumed to be near equilibrium (Lozano et al. 2008). For an initial degree of saturation of 0.25, the normalized vapor concentration soon after the start of heating was smaller than this limit and decreased to 0.63 at the end of the heating period, indicating that use of a the nonequilibrium model was justified. For an initial degree of saturation of 0.5, the normalized vapor concentration was 0.82 soon after the start of heating and remained above 0.75 indicating that the equilibrium assumption may be valid for initially wetter soils. The time series in Fig. 12(a) indicate that the phase change process did not reach steady state conditions by the end of the heat injection period. Horizontal profiles of the normalized vapor concentrations at the end of heating shown in Fig. 12(b) indicate that lower vapor concentrations were present near the heat source and had a similar zone of influence to the degree of saturation in Fig. 7(b). Despite the higher magnitudes of normalized vapor concentration, greater changes in normalized vapor concentration with horizontal distance are observed for the initially wetter soil ($S_{r0} = 0.5$), which may be the reason for the greater change in degree of saturation at this location. Vertical profiles of normalized vapor concentration at the end in Fig. 12(c) are similar to those for the degree of saturation in Fig. 8(b). A relatively high vapor concentration was observed close to the surface because of the lower initial degrees of saturation and higher temperatures, and also because of the upward movement of water vapor due to buoyancy effects.

Horizontal profiles of latent heat transfer due to phase change for soils with initial degrees of saturation of 0.25 and 0.50 are shown in Fig. 13(a). While latent heat transfer was higher near the heat source indicating evaporation, a very slight value of under zero was observed at a distance about 1 m away from the heat exchanger, indicating that condensation is occurring in the soil further from the heat source. A comparison between the total thermal energy injected into the geothermal heat exchanger along with the heat transferred within the soil by latent heat transfer is shown in Fig. 13(b). The total energy injected was 180 MJ at the end of 90 days of heating while the energy transferred by latent heat transfer was 44 MJ, which is approximately 24% of the total heat injected into the system. This is an appreciable amount and further justifies the need to accurately account for nonequilibrium effects. The remaining thermal energy was transferred due to a combination of conduction and convection associated with vapor diffusion.

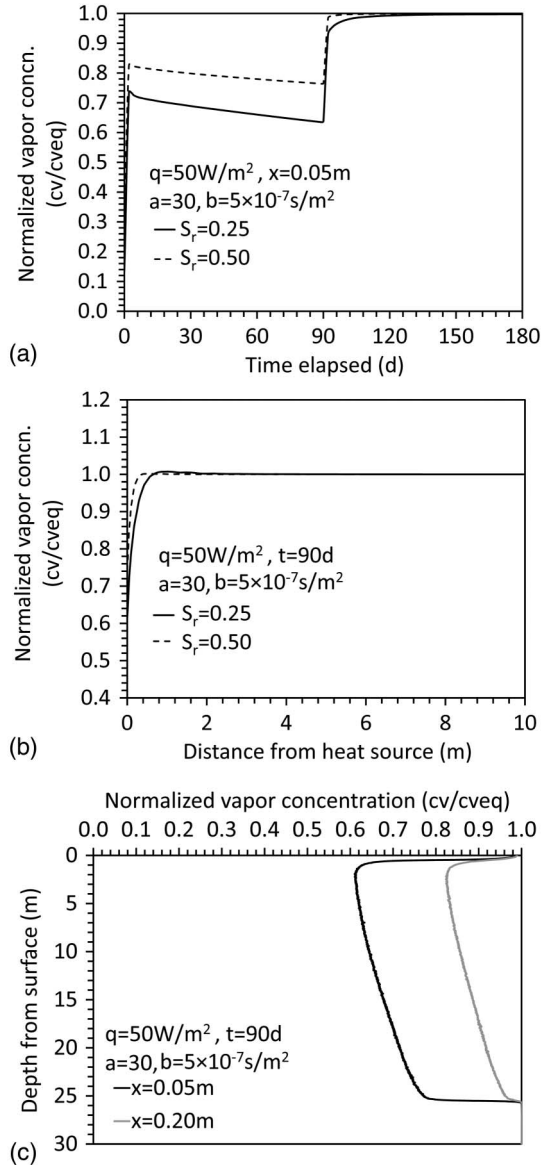

Fig. 12. Vapor concentrations normalized by the equilibrium vapor concentration: (a) time series; (b) horizontal profiles at the end of heating; and (c) vertical profiles at the end of heating.

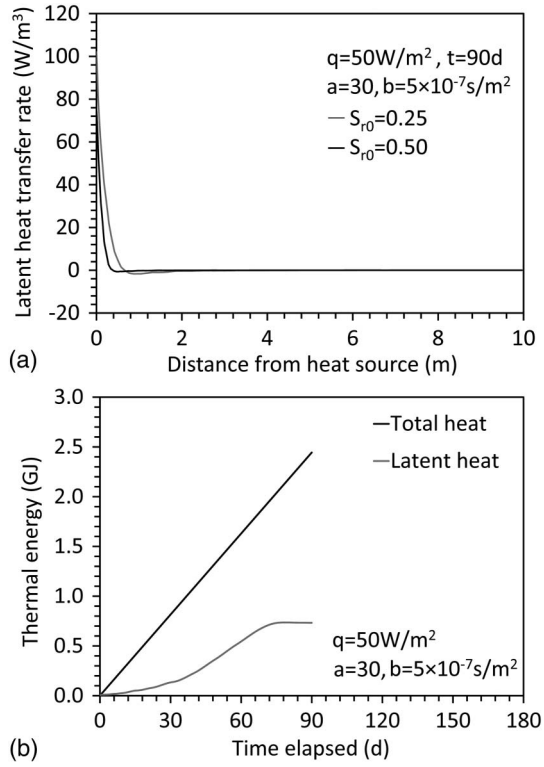

Fig. 13. (a) Distributions of latent heat transfer rate at the end of heating at depths corresponding to initial degrees of saturation of 0.25 and 0.50; (b) comparison of the total heat injected with the energy transferred due to phase change.

Conclusions

A model that includes a recently-developed set of thermohydraulic constitutive relationships was calibrated for a silt soil to understand the roles of vapor diffusion and phase change on the coupled heat transfer and water flow in a fine-grained, nondeformable unsaturated soil layer initially under hydrostatic conditions surrounding a geothermal heat exchanger during heat injection and ambient cooling. In general, the modeling results confirm the importance of considering vapor diffusion and phase change in simulations of geothermal heat exchangers in unsaturated soils, as well as the relevance of considering nonequilibrium phase change in initially drier soil layers. Although quantitative conclusions from the simulations are specific to the given soil and geometry investigated, several key conclusions can be drawn regarding the use of geothermal heat exchangers in thermal energy storage systems in unsaturated soils, including:

- The greater rate of increase in temperature observed in a model that includes enhanced vapor diffusion and phase change indicates that conduction-only design models may underestimate the transient increase in temperature in a thermal energy storage system in the vadose zone.
- The rate of heat dissipation during an ambient cooling period was slower when considering vapor diffusion and phase change due to the drying observed during heat injection. The drying can be considered permanent for practical purposes within the time frame of the ambient cooling cycle. This may be partially because the decrease in hydraulic conductivity during the thermally induced drying led to a negligible amount of liquid water flow back toward the heat exchanger during ambient cooling.
- Although reductions in both thermal conductivity and volumetric heat capacity are observed during thermally induced drying of the soil surrounding the geothermal heat exchanger, the percentage reductions in thermal conductivity were greater. This indicates that a lower rate of heat dissipation during ambient cooling can be expected in unsaturated soils, but the maximum possible heat stored will not decrease by as large of an amount.
- The zone of influence of changes in temperature was observed to be greater than the zone of influence of the changes in degree of saturation for the soil under investigation, but both zones of influence are appreciable enough that overlap is expected in thermal energy storage systems with closely-spaced geothermal heat exchangers (i.e., 1.5–2.0 m).
- The normalized vapor concentrations in the initially drier soils near the ground surface were below the limit at which nonequilibrium phase change is expected to occur, justifying the use of this more advanced modeling approach. The vapor concentration gradient was greater in the initially wetter soils deeper in the profile

- The initial degree of saturation was observed to influence both heat transfer and water flow in the model with vapor diffusion and phase change with the greatest change in the degree of saturation occurring for soil with initially higher degrees of saturation.

Acknowledgments

Funding from National Science Foundation grant CMMI 1230237 is much appreciated. The opinions are those of the authors alone and do not reflect the viewpoint of the sponsor.

References

Acuña, J., M. Fossa, P. Monzó, and B. Palm. 2012. "Numerically generated G-functions for ground coupled heat pump applications." In *Proc., COMSOL Multiphysics Conf., Milan*, 1–6. Brescia, Italy: COMSOL.

Armstrong, J. E., E. O. Frind, and R. D. McClellan. 1994. "Nonequilibrium mass transfer between the vapor, aqueous, and soil-phases in unsaturated soils during vapor extraction." *Water Resour. Res.* 30 (2): 355–368. https://doi.org/10.1029/93WR02481.

Baladi, J. Y., D. L. Ayers, and R. J. Schoenhals. 1981. "Transient heat and mass transfer in soils." *Int. J. Heat Mass Transfer.* 24 (3): 449–458. https://doi.org/10.1016/0017-9310(81)90053-3.

Başer, T., Y. Dong, N. Lu, and J. S. McCartney. 2016a. "Role of considering non-constant soil thermal parameters in the simulation of geothermal heat storage systems in the vadose zone." In *Challenges and Innovations in Geotechnics: Proc., 8th Asian Young Geotechnical Engineers Conf.*, edited by A. Zhussupbekov, 137–142. Boca Raton, FL: CRC Press.

Başer, T., N. Lu, and J. S. McCartney. 2016b. "Operational response of a soil-borehole thermal energy storage system." *J. Geotech. Geoenviron. Eng.* 142 (4): 04015097. https://doi.org/10.1061/(ASCE)GT.1943-5606.0001432.

Başer, T., T. Traore, and J. S. McCartney. 2016c. "Physical modeling of coupled heat transfer and water flow in soil-borehole thermal energy storage systems in the vadose zone." In *Geothermal energy: An important resource*, edited by C. B. Dowling, L. J. Florea, and K. Neumann, eds., 81–93. Boulder, CO: GSA Books.

Bear, J. 1972. *Dynamics of fluids in porous media*, 764. Mineola, NY: Dover.

Beier, R. A., J. Acuña, P. Mogensen, and B. Palm. 2014. "Transient heat transfer in a coaxial borehole heat exchanger." *Geothermics* 51 (Jul): 470–482. https://doi.org/10.1016/j.geothermics.2014.02.006.

Bénet, J. C., and P. Jouanna. 1982. "Phenomenological relation of phase change of water in a porous-medium-experimental verification and measurement of the phenomenological coefficient." *Int. J. Heat Mass Trans.* 25 (11): 1747–1754. https://doi.org/10.1016/0017-9310(82)90154-5.

Bénet, J. C., A. L. Lozano, F. Cherblanc, and B. Cousin. 2009. "Phase change of water in a hygroscopic porous medium: Phenomenological relation and experimental analysis for water in soil." *J. Non-Equilibr. Thermodyn.* 34 (2): 133–153. https://doi.org/10.1515/JNETDY.2009.008.

Bixler, N. E. 1985. *NORIA: A finite element computer program for analyzing water, vapor, air and energy transport in porous media*. SAND84-2057. Albuquerque, NM: Sandia National Laboratories.

Bouyoucos, G. J. 1915. "Effect of temperature on movement of water vapor and capillary moisture in soils." *J. Agric. Res.* 5 (4): 141–172.

Campbell, G. S. 1985. *Soil physics with BASIC: Transport models for soil–plant systems*. New York: Elsevier.

Campbell, G. S., J. D. Jungbauer, W. R. Bidlake, and R. D. Hungerford. 1994. "Predicting the effect of temperature on soil thermal conductivity." *Soil Sci.* 158 (5): 307–313. https://doi.org/10.1097/00010694-199411000-00001.

Cass, A., G. S. Campbell, and T. L. Jones. 1984. "Enhancement of thermal water vapor diffusion in soil." *Soil Sci. Soc. Am.* 48 (1): 25–32. https://doi.org/10.2136/sssaj1984.03615995004800010005x.

Catolico, N., S. Ge, and J. S. McCartney. 2016. "Numerical modeling of a soil-borehole thermal energy storage system." *Vadose Zone J.* 15 (1): 1–17. https://doi.org/10.2136/vzj2015.05.0078.

Chammari, A., B. Naon, F. Cherblanc, B. Cousin, and J. C. Bénet. 2008. "Interpreting the drying kinetics of a soil using a macroscopic thermodynamic nonequilibrium of water between the liquid and vapor phase." *Drying Technol.* 26 (7): 836–843. https://doi.org/10.1080/07373930802135998.

Chapuis, S., and M. Bernier. 2009. "Seasonal storage of solar energy in borehole heat exchangers." In *Proc. IBPSA Conf. Building Simulations*, 599–606. Toronto: IBPSA.

Ciriello, V., M. Bottarelli, V. Di Federico, and D. M. Tartakovsky. 2015. "Temperature fields induced by geothermal devices." *Energy* 93 (2): 1896–1903. https://doi.org/10.1016/j.energy.2015.10.052.

Claesson, J., and G. Hellström. 1981. "Model studies of duct storage systems." *New energy conservation technologies and their commercialization*, edited by J. P. Millhone and E. H. Willis, eds., 762–778. Berlin, Germany: Springer.

Cleall, P. J., S. C. Seetharam, and H. R. Thomas. 2007. "Inclusion of some aspects of chemical behaviour of unsaturated soil in thermo/hydro/chemical/mechanical models. I: Model development." *J. Eng. Mech.* 133 (3): 338–347. https://doi.org/10.1061/(ASCE)0733-9399(2007)133:3(338).

Cleall, P. J., R. M. Singh, and H. R. Thomas. 2011. "Non-isothermal moisture movement in unsaturated kaolin: An experimental and theoretical investigation." *Geotech. Test. J.* 34 (5): 514–524. https://doi.org/10.1520/GTJ103585.

Côté, J., and J. M. Konrad. 2005. "Thermal conductivity of base course materials." *Can. Geotech. J.* 42 (1): 61–78. https://doi.org/10.1139/cgj-2017-0447.

Dong, Y., J. S. McCartney, and N. Lu. 2015. "Critical review of thermal conductivity models for unsaturated soils." *Geotech. Geol. Eng.* 33 (2): 207–221. https://doi.org/10.1007/s10706-015-9843-2.

Eskilson, P. 1987. *Thermal analysis of heat extraction boreholes*. Lund, Sweden: Lund Univ.

Ewen, J. 1988. "Thermal instability in gently heated unsaturated sand." *Int. J. Heat Mass Transfer* 31 (8): 1701–1710. https://doi.org/10.1016/0017-9310(88)90282-7.

Ewen, J., and H. R. Thomas. 1989. "Heating unsaturated medium sand." *Géotechnique* 39 (3): 455–470. https://doi.org/10.1680/geot.1989.39.3.455.

Farouki, O. T. 1981. *Thermal properties of soils. Monograph 81-1*, 136. Hanover, New Hampshire: U.S. Army Cold Regions Research and Engineering Laboratory Hanover.

Gehlin, S. 2002. "Thermal response test: Method development and evaluation." Doctoral thesis, Lulea Univ. of Technology.

Gens, A., A. Garcia Molina, S. Olivella, E. E. Alonso, and F. Huertas. 1998. "Analysis of a full scale in-situ test simulating repository conditions." *Int. J. Numer. Anal. Methods Geomech.* 22 (7): 515–548. https://doi.org/10.1002/(SICI)1096-9853(199807)22:7<515::AID-NAG926>3.0.CO;2-8.

Gens, A., M. Sánchez, L. Guimarães, E. E. Alonso, A. Lloret, S. Olivella, M. V. Villar, and F. Huertas. 2009. "A full scale in situ heating test for high level nuclear waste disposal: Observations, analysis and interpretation." *Géotechnique* 59 (4): 377–399. https://doi.org/10.1680/geot.2009.59.4.377.

Gens, A., J. Vaunat, B. Garitte, and Y. Wileveau. 2007. "In situ behaviour of a stiff layered clay subject to thermal loading: Observations and interpretation." *Géotechnique* 57 (2): 207–228. https://doi.org/10.1680/geot.2007.57.2.207.

Grant, S. A., and A. Salehzadeh. 1996. "Calculations of temperature effects on wetting coefficients of porous solids and their capillary pressure functions." *Water Resour. Res.* 32 (2): 261–270. https://doi.org/10.1029/95WR02915.

Guimarães, L. D., A. Gens, M. Sánchez, and S. Olivella. 2013. "A chemo-mechanical constitutive model accounting for cation exchange in expansive clays." *Géotechnique* 63 (3): 221–234. https://doi.org/10.1680/geot.SIP13.P.012.

Guimarães, L. M., A. Gens, and S. Olivella. 2007. "Coupled thermo-hydro-mechanical and chemical analysis of expansive clay subjected to

heating and hydration." *Transp. Porous Media* 66 (3): 341–372. https://doi.org/10.1007/s11242-006-0014-z.
Gurr, C. G., T. J. Marshall, and J. T. Hutton. 1952. "Movement of water in soil due to a temperature gradient." *Soil Sci.* 74 (5): 335–346. https://doi.org/10.1097/00010694-195211000-00001.
Hillel, D. 1980. *Fundamental of soil physics*. San Diego, CA: Academic Press.
Ingersoll, L. R., and H. J. Plass. 1948. "Theory of the ground pipe heat source for the heat pump." *ASHVE Transactions* 54: 119–122.
Ingersoll, L. R., O. J. Zobel, and A. C. Ingersoll. 1954. *Heat conduction with engineering, geological, and other applications*, 325. Revised ed. Madison, WI: Univ. of Wisconsin Press.
Kavanaugh, S. P. 1998. "Design method for hybrid ground-source heat pumps." *ASHRAE Transact.* 104 (2): 691–698.
Lamarche, L., and B. Beauchamp. 2007. "A new contribution to the finite line-source model for or geothermal boreholes." *Energy Build.* 39 (2): 188–198. https://doi.org/10.1016/j.enbuild.2006.06.003.
Lide, D. R., ed. 2001. *Handbook of chemistry and physics*. Boca Raton, FL: CRC Press.
Lozano, A. L., F. Cherblanc, B. Cousin, and J. C. Benet. 2008. "Experimental study and modelling of the water phase change kinetics in soils." *Eur. J. Soil Sci.* 59 (5): 939–949. https://doi.org/10.1111/j.1365-2389.2008.01050.x.
Lu, N., and Y. Dong. 2015. "A closed form equation for thermal conductivity of unsaturated soils at room temperature." *J. Geotech. Geoenviron. Eng.* 141 (6): 04015016. https://doi.org/10.1061/(ASCE)GT.1943-5606.0001295.
McCartney, J. S., T. Başer, N. Zhan, N. Lu, S. Ge, and K. Smits. 2017. "Storage of solar thermal energy in borehole thermal energy storage systems." *IGSHPA Technical Conf. and Expo*, 1–8. Leeds, UK: University of Leeds.
McCartney, J. S., S. Ge, A. Reed, N. Lu, and K. Smits. 2013. "Soil-borehole thermal energy storage systems for district heating." In *Proc., European Geothermal Congress 2013*, 1–10. Brussels, Belgium: European Geothermal Energy Council.
Millington, R. J., and J. M. Quirk. 1961. "Permeability of porous solids." *Trans. Faraday Soc.* 57: 1200–1207. https://doi.org/10.1039/tf9615701200.
Monteith, J. L., and M. H. Unsworth 1990. *Principles of environmental physics*. New York: Routledge Chapman and Hall.
Moradi, A. M., K. Smits, N. Lu, and J. S. McCartney. 2016. "3-D experimental and numerical investigation of heat transfer in unsaturated soil with an application to soil borehole thermal energy storage (SBTES) systems." *Vadose Zone J.* 15 (10): 1–17. https://doi.org/10.2136/vzj2016.03.0027.
Moradi, A. M., K. Smits, J. Massey, A. Cihan, and J. S. McCartney. 2015. "Impact of coupled heat transfer and water flow on soil borehole thermal energy storage (SBTES) systems: Experimental and modeling investigation." *Geothermics* 57 (Sep): 56–72. https://doi.org/10.1016/j.geothermics.2015.05.007.
Nordell, B., and G. Hellström. 2000. "High temperature solar heated seasonal storage system for low temperature heating of buildings." *Solar Energy* 69 (6): 511–523.
Olivella, S., A. Gens, J. Carrera, and E. E. Alonso. 1996. "Numerical formulation for a simulator (CODE-BRIGHT) for the coupled analysis of saline media." *Eng. Comput.* 13 (7): 87–112. https://doi.org/10.1108/02644409610151575.
Ozudogru, T. Y., O. Ghasemi-Fare, C. G. Olgun, and P. Basu. 2015. "Numerical modeling of vertical geothermal heat exchangers using finite difference and finite element techniques." *Geotech. Geol. Eng.* 33 (2): 291–306. https://doi.org/10.1007/s10706-014-9822-z.
Penman, H. L. 1940. "Gas and vapor movement in soil: I. The diffusion of vapors in porous solids." *J. Agric. Sci.* 30 (03): 437–462. https://doi.org/10.1017/S0021859600048164.
Philip, J. R., and D. A. de Vries. 1957. "Moisture movement in porous materials under temperature gradients." *Trans. Am. Geophys. Union* 38 (2): 222–232. https://doi.org/10.1029/TR038i002p00222.
Saito, H., J. Simunek, and B. P. Mohanty. 2006. "Numerical analysis of coupled water, vapor, and heat transport in the vadose zone." *Vadose Zone J.* 5 (2): 784–800. https://doi.org/10.2136/vzj2006.0007.
Shah, D. J., J. W. Ramsey, and M. Wang. 1984. "An experimental determination of the heat and mass transfer coefficients in moist, unsaturated soils." *Int. J. Heat Mass Transfer* 27 (7): 1075–1085. https://doi.org/10.1016/0017-9310(84)90123-6.
Sibbitt, B., D. McClenahan, R. Djebbar, J. Thornton, B. Wong, J. Carriere, and J. Kokko. 2012. "The performance of a high solar fraction seasonal storage district heating system—Five years of operation." *Energy Procedia* 30: 856–865. https://doi.org/10.1016/j.egypro.2012.11.097.
Smith, W. O. 1943. "Thermal transfer of moisture in soils." *Am. Geophys. Union Trans.* 24 (2): 511–524. https://doi.org/10.1029/TR024i002p00511.
Smits, K. M., A. Cihan, S. Sakaki, and T. H. Illangasekare 2011. "Evaporation from soils under thermal boundary conditions: Experimental and modeling investigation to compare equilibrium- and nonequilibrium-based approaches." *Water Resour. Res.* 47: W05540. https://doi.org/10.1029/2010WR009533.
Smits, K. M., S. Sakaki, S. E. Howington, J. F. Peters, and T. H. Illangasekare. 2013. "Temperature dependence of thermal properties of sands across a wide range of temperatures (30–70 °C)." *Vadose Zone J.* 21 (1): 1–8. https://doi.org/10.2136/vzj2012.0033.
Tarn, J. Q., and Y. M. Wang. 2004. "End effects of heat conduction in circular cylinders of functionally graded materials and laminated composites." *Int. J. Heat Mass Transfer* 47 (26): 5741–5747. https://doi.org/10.1016/j.ijheatmasstransfer.2004.08.003.
Thomas, H. R., and Y. He. 1997. "A coupled heat-moisture transfer theory for deformable unsaturated soil and its algorithmic implementation." *Int. J. Numer. Methods Eng.* 40 (18): 3421–3441. https://doi.org/10.1002/(SICI)1097-0207(19970930)40:18<3421::AID-NME220>3.0.CO;2-C.
Thomas, H. R., Y. He, M. R. Sansom, and C. L. W. Li. 1996. "On the development of a model of the thermo-mechanical-hydraulic behavior of unsaturated soils." *Eng. Geol.* 41 (1–4): 197–218. https://doi.org/10.1016/0013-7952(95)00033-X.
Thomas, H. R., and S. D. King. 1991. "Coupled temperature capillary potential variations in unsaturated soil." *J. Eng. Mech.* 117 (11): 2475–2491. https://doi.org/10.1061/(ASCE)0733-9399(1991)117:11(2475).
Thomas, H. R., M. Sansom, and S. W. Rees. 2001. "Non-isothermal flow." *Environmental Geomechanics*, 131–169. Vienna, Austria: Springer.
Thomas, H. R., and M. R. Sansom. 1995. "Fully coupled analysis of heat, moisture and air transfer in unsaturated soil." *J. Eng. Mech.* 121 (3): 392–405. https://doi.org/10.1061/(ASCE)0733-9399(1995)121:3(392).
Trautz, A. C., K. M. Smits, and A. Cihan. 2015. "Continuum-scale investigation of evaporation from bare soil under different boundary and initial conditions: An evaluation of nonequilibrium phase change." *Water Resour. Res.* 51 (9): 7630–7648. https://doi.org/10.1002/2014WR016504.
van Genuchten, M. T. 1980. "A closed-form equation for predicting the hydraulic conductivity of unsaturated soils." *Soil Sci. Soc. Am. J.* 44 (5): 892–898. https://doi.org/10.2136/sssaj1980.03615995004400050002x.
Wayllace, A., and N. Lu. 2012. "A transient water release and imbibitions method for rapidly measuring wetting and drying soil water retention and hydraulic conductivity functions." *Geotech. Test. J.* 35 (1): 103–117. https://doi.org/10.1520/GTJ103596.
Welsch, B., W. Rühaak, D. O. Schulte, K. Bär, S. Homuth, and I. Sass. 2015. "Comparative study of medium deep borehole thermal energy storage systems using numerical modelling." In *Proc., World Geothermal Congress 2015*, 1–6. Bochum, Germany: International Geothermal Association.
Whitaker, S. 1977. "Simultaneous heat, mass and momentum transfer in porous media: A theory of drying porous media." *Adv. Heat Transf.* 13: 119–203. https://doi.org/10.1016/S0065-2717(08)70223-5.
Yavuzturk, C. 1999. "Modeling of vertical ground loop heat exchangers for ground source heat pump systems." Ph.D. thesis, Oklahoma State Univ.
Zhang, J., and A. K. Datta. 2004. "Some considerations in modeling of moisture transport in heating of hygroscopic materials." *Drying Technol.* 22 (8): 1983–2008. https://doi.org/10.1081/DRT-200032740.